*35th EPS Conference on Plasma Phys. Hersonissos, 9 - 13 June 2008 ECA Vol.**32D**, P-5.055 (2008)*

Investigation of fast ion behavior in burning plasmas via Ion Cyclotron Resonance Heating

C. Di Troia, S. Briguglio, G. Calabrò, A. Cardinali, F. Crisanti,
G. Fogaccia, M. Marinucci, G. Vlad, F. Zonca
Associazione Euratom-ENEA sulla Fusione, C.R. Frascati,
C.P. 65 - I-00044 - Frascati, Rome, Italy

In this work we have analyzed the behavior and studied the transport and confinement of fast (MeV) ions produced by Ion Cyclotron Resonance Heating (ICRH) in magnetically confined burning plasmas. Simulations have been performed by HMGC [1], a hybrid MHD-particle 3-D simulation code that properly takes into account kinetic effects and nonlinear dynamics by means of a Particle In Cell approach. This code has been recently extended to handle the case of an anisotropic Maxwellian velocity space fast ion distribution function, such as that expected for ICRH.

We analyze the case of FAST (Fusion Advanced Studies Torus) [2] conceptual design, conceived to simultaneously address crucial physics issues in burning plasma, including energetic particle excitations of collective meso-scale fluctuations belonging to the Alfvén spectrum and their cross-scale couplings with micro-scale turbulence. We have used the JETTO code [3], a predictive 1.5-D transport code which uses a semi-empirical mixed Bohm/gyro-Bohm transport model [4], to compute the evolution of a time dependent axisymmetric MHD equilibrium, summarized in Table 1. Then, the 2D full-wave code TORIC is used in combination with the SSQLFP code, which solves the quasi-linear Fokker-Planck equation in 2D velocity space [5], to obtain the effective temperature and density of the minority ion tail (^{3}He in D plasma).

The Alfvén fluctuation spectrum in FAST is expected to be dominated by the same toroidal mode numbers ($15 \lesssim n \lesssim 25$) that will be relevant in ITER and to have the same frequencies expressed in units of the Alfvén frequency. Investigating linear and nonlinear dynamics of $15 \lesssim n \lesssim 25$ Alfvénic oscillations is very demanding in terms of computational resources: these analyses will represent a significant part of FAST theory and modeling activities. In the present work, we have limited our investigations of high-n modes to few paradigmatic cases (see below) and concentrated our analyses to moderate mode numbers. Because of the relevance of the interactions between modes and trapped particles, dominated by precession and precession-bounce resonances, the long wavelength limit (moderate-n) is expected to favor low-frequency fishbone-like modes [6].

Fishbone modes are known to be $n = 1$ internal kink oscillations excited by a magnetically

$R_0 = 1.82\ m$	$a = 0.64\ m$	$n_{e0}(n_{i0}) = 2.5\times10^{20} m^3$	$B = 7.4\ T$	$I_{tor} = 6500\ kA$
$(A_i, Z_i) = (2,1)$	$(A_H, Z_H) = (3,2)$	$n_{H,max}/n_{i0} = 0.006$	$T_{e0}(T_{i0}) = 11\ keV$	$T_{H,max} = 0.65\ MeV$
$q(0) = q_{min} = 1.1$	$q(a) = 3.5$	$P_{ICRH} = 30MW$	$\omega_{ICRH} = 67\ MHz$	$r_{ICRH}/a = 0.35$

Table 1: Reference FAST Equilibrium Scenario

trapped population of fast particles [7, 8]. More generally, Energetic Particle Modes (EPM) [9] can be excited by energetic particle characteristic motions in a broad range of mode numbers and frequencies [9, 10]. Since perturbations of the shear Alfvén wave spectrum generally consist of singular (inertial) and regular (ideal MHD) structures, it is always possible to derive their dispersion relation in a fishbone-like form $i\Lambda(\omega) = \delta\hat{W}_f + \delta\hat{W}_k$ [9, 10, 11]. Here, $i\Lambda(\omega)$ [11, 12] is the inertial layer contribution due to thermal ions, while the right hand side comes from background MHD ($\delta\hat{W}_f$) and energetic particle ($\delta\hat{W}_k$) contributions in the regular ideal regions. For $|q\omega/\omega_A| \ll 1$, with $\omega_A = v_A/R_0$ the Alfvén frequency, v_A the Alfvén speed and q the safety factor, and neglecting thermal ion kinetic effects [12] for consistency with the hybrid model employed by the HMGC code [1], we have [13, 14] $\Lambda = q\omega/\omega_A$, while $\delta\hat{W}_k \propto \beta_H$.

Low frequency EPMs exhibit the same bursting nature of $n = 1$ fishbones and are characterized by the same wave-particle resonance excitation mechanism: thus, they can be quoted moderate-n fishbone-like modes [15]. At marginal stability, fishbone-like EPMs are characterized by $\delta\hat{W}_f + \mathbf{R}\mathrm{e}\delta\hat{W}_k \simeq 0$ [9], which determines the real mode frequency to be essentially that of the characteristic particle motions. Furthermore, the growth rate is given by the condition $\gamma = (-\partial\mathbf{R}\mathrm{e}\delta\hat{W}_k/\partial\omega)^{-1}(\mathbf{I}\mathrm{m}\delta\hat{W}_k - q\omega/\omega_A)$. Since $\omega \simeq \bar{\omega}_{dH} \propto T_H$ for the precession resonance and $\mathbf{I}\mathrm{m}\delta\hat{W}_k \propto \beta_H$, the EPM marginal stability condition sets a critical energetic ion density for resonant mode excitation, as for the $n = 1$ fishbone [7]. Meanwhile, the mode growth rate is expected to increase linearly with the fast ion density near marginal stability.

Figure 1 shows the results of several simulations related to a monotonic q scenario for FAST, whose main parameters are summarized in Table 1. The initial fast ion distribution function has been assumed a bi-Maxwellian with Lorentzian temperature profiles and Gaussian density profile, centered at r_{ICRH} consistent with TORIC output profiles. The peak temperatures are $T_\perp = 650\ keV$ and $T_\parallel = 60\ keV$. Numerical simulations have been performed for different toroidal mode numbers n. Moreover, while keeping the shape of the density profile fixed, the fast-ion density has been artificially increased by rescaling the reference scenario value by a factor σ. Values of the linear growth rate for such simulations are reported in Fig. 1 (left). In particular, cases with $n = 8$ and different values of σ are considered, along with cases with $\sigma = 8$ and different values of n. We observe that the instability of the system increases with n,

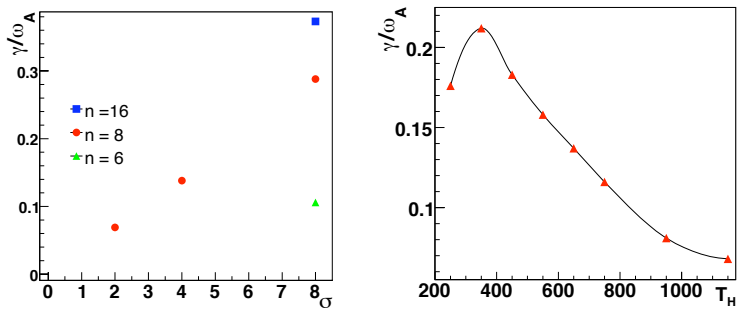

Figure 1: Left: normalized growth rate of the most unstable modes, γ/ω_A, vs. σ, for $n = 6$ (triangle), $n = 8$ (circles) and $n = 16$ (square). Right: mode growth rate versus $T_\perp$ for $n = 8$.

as expected in this moderate toroidal number regime. Note that both larger n and lower σ simulations have not been performed, at this preliminary stage, because of computational resource limitations.

In Fig. 1 (right), the growth rate is reported versus the fast-ion $T_\perp$ for $n = 8$ simulations characterized by the same value of the fast-ion pressure (four times the reference scenario value) and fixed ratio $T_\perp/T_\parallel$. The presence of an instability peak is observed. Note that the peak for $n = 8$ occurs at lower $T_\perp$ than the value ($T_\perp \simeq 600 - 700keV$) expected for the most unstable mode numbers, $15 \lesssim n \lesssim 25$.

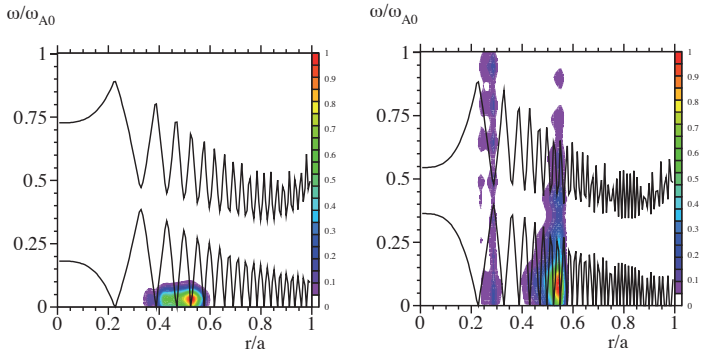

Figure 2: Power spectra for $n = 8$, $\sigma = 2$ (left) and $n = 16$, $\sigma = 1$ (right) simulations, with the other parameters as in the reference scenario. The upper and lower continua are also shown (black curves).

Figure 2 compares the power spectra obtained during the linear growth phase in $n = 8$ and $n = 16$ simulations. We see that the larger-n case shows a much richer spectrum of modes [15]. Finite-orbit and collective-dynamics effects on the fast-ion transport are shown in Fig. 3 for a $n = 8$ simulation. The initial local (zero orbit width) pressure profile (left) is compared with that obtained after fast-ion unperturbed motion has modified their distribution function because

of finite-orbit effects (centre) and that produced by the nonlinear interaction with the unstable modes (right). These results confirm that in reactor relevant burning plasmas the Alfvén fluctuation spectrum will be dominated by a dense spectrum of modes with characteristic frequencies and radial localizations [15], which cause rich nonlinear dynamics with potential detrimental impact on fast particle transport. The role of such modes on the overall fusion performance and their cross-scale couplings with micro-turbulence and thermal plasma transport [11] will be the subject of future investigations.

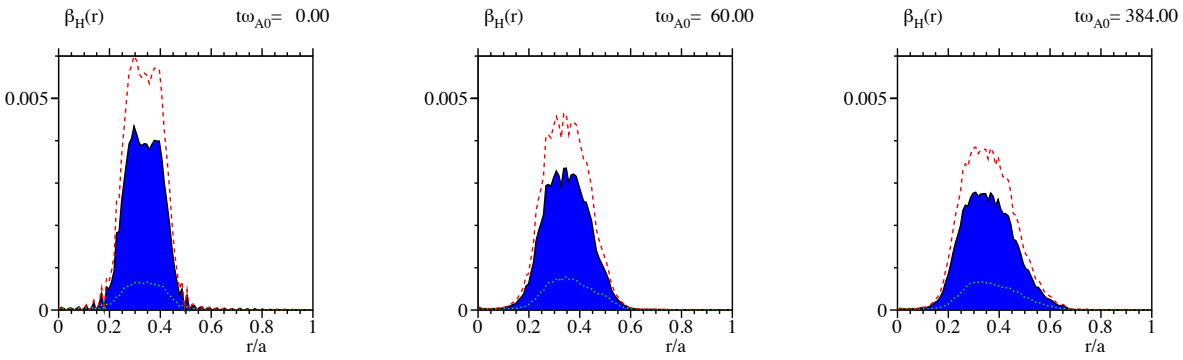

Figure 3: Fast-ion pressure profiles at three different times (cf. the text) for a $n = 8$, $\sigma = 2$ simulation. Dotted curves represent perpendicular (red) and parallel (green) pressures.

References

[1] S. Briguglio, G. Vlad, F. Zonca, and C. Kar, Phys. Plasmas **2**, 3711, (1995).

[2] A. Pizzuto et al, ENEA Technical Report FUS-FAST-RTI-07-001 (2007)

[3] G. Cenacchi and A. Taroni 1988 JETTO: A free boundary plasma transport code (basic version); report JET-IR (88) 03

[4] G. Vlad et al., Nucl. Fusion, Vol. 38 (1998), 557

[5] M. Brambilla, Plasma Physics and Controlled Nuclear Fusion **41**, 1 (1999)

[6] G. Vlad, S. Briguglio, G. Fogaccia, F. Zonca and M. Scheider, Nucl. Fusion **46**, 1, (2006).

[7] L. Chen, R.B. White and M.N. Rosenbluth, Phys. Rev. Lett. **52**, 1122, (1984)

[8] B. Coppi and F. Porcelli, Phys. Rev. Lett. **57**, 2272, (1986)

[9] L. Chen, Phys. Plasmas **1**, 1519, (1994)

[10] S. T. Tsai and L. Chen, Phys. Fluids B **5**, 3284 (1993).

[11] F. Zonca and L. Chen, Plasma Phys. Control. Fusion **48**, 537, (2006)

[12] F. Zonca, L. Chen and R.A. Santoro, Plasma Phys. Control. Fusion **38**, 2011, (1996)

[13] F. Zonca and L. Chen, Phys. Plasmas **7**, 4600, (2000).

[14] F. Zonca et al., Phys. Plasmas **9**, 4939, (2002).

[15] L. Chen and F. Zonca, Nucl. Fusion **47**, S727, (2007)